

**Military Technical College  
Kobry El-Kobbah,  
Cairo, Egypt.**



**13<sup>th</sup> International Conference  
on Applied Mechanics and  
Mechanical Engineering.**

## **COMPARATIVE STUDY OF INITIATION FATIGUE LIFE OF FREE DEFECT AND DEFECTIVE MATERIALS**

BOURAOU<sup>1</sup> Ch., NASR<sup>1,2</sup> A., NADOT<sup>2</sup> Y. and FATHALLAH<sup>3</sup> R.

### **ABSTRACT**

This paper presents an experimental comparison of crack initiation, between free defect and defect material, under High Cycle Fatigue (HCF) loading. Experiments are carried out on a C35 steel. Results show that crack initiation and crack propagation mechanisms for defective material are the same as defect free material: cracks are initiated in the maximum shear plane then they propagate in the plane perpendicular to the maximum principal stress direction. But the length of the stage I cracks of defect materials is always very short in comparison with those of defect free materials. Crack propagation regime life in defect materials is very short, contrary to defect free material which shows an early crack initiation. However, contrary to the common belief, the fatigue life initiation is not consumed in defective material and particularly in torsion loading where the cyclic stress tensor becomes complex around the defect.

### **KEY WORDS**

Fatigue; crack initiation; crack propagation ; material defect.

---

<sup>1</sup> Laboratoire de Génie Mécanique, Ecole Nationale d'Ingénieurs de Monastir, Avenue Ibn El Jazzar, 5019 Monastir, Tunisia Mail : chokri.bouraoui@enim.rnu.tn

<sup>2</sup> Laboratoire de Génie Mécanique, Institut supérieur de transport et de la logistique, 4000 Sousse, Tunisia

<sup>3</sup> Laboratoire de Mécanique et de Physique des Matériaux, UMR CNRS no. 6617, ENSMA, Téléport 2, BP 40 109, 86961 Futuroscope Cedex, France

## INTRODUCTION

Defects such as surface flaws or non-metallic inclusions are often the origin of cracks leading to a reduction of the fatigue strength. Therefore, the evaluation of the effects of small defects on the fatigue strength often has an important design consideration.

Many experiments have been mainly conducted on artificial surface defects such as cylindrical drill holes [1], [3], [4], spherical and elliptical defect [2]. Experimental data concerning natural defects and particularly internal ones are not numerous. Tests have been carried out by Nadot [6] to study the influence of natural internal and surface defects on the fatigue limit of defective nodular cast iron.

Murakami et al. [1], [5] proposed an approach based on experimental results. Indeed, an interesting geometrical parameter,  $\sqrt{area}$ , which is the square root of the projected area of the defect on the plane perpendicular to the direction of the maximal principal stress [1]. This parameter is used to model the defect size. This approach suggests a simple relationship between the fatigue limit and this size parameter. Their estimations of the fatigue limit for various metallic materials were good. This empirical criterion gives good results for spherical-type defects. Other approaches based on notch effect or cracks have been proposed and a comparison is done by Nadot [6]. These approaches are often limited to uniaxial alternated loading so that they cannot be used in the case of multiaxial loading. The approach developed by Nadot et al. [7] is based on the stress gradient around the defect. This criterion has been largely validated for different morphologies and sizes of defect .

In this paper, an experimental comparison of fatigue life initiation and fatigue life propagation of defective and defect free material is presented. In order to understand the influence of the defect on the fatigue life initiation, spherical defects have been introduced at the surface of specimens made in low carbon steel. SEM observations have been done to describe initiation mechanisms. Defect free material behaviour is compared to defective one.

## MATERIAL AND EXPERIMENTAL DETAILS

The studied material is a low carbon steel C35, used in many industrial applications. The mechanical characteristics are given in Table 1. This steel shows an alternance of ferrite and pearlite bands, and the mean grain size is 16  $\mu\text{m}$  for ferrite and 22  $\mu\text{m}$  for pearlite.

All the specimens were polished before fatigue testing in order to remove machining marks and to observe crack initiation and early propagation. Then artificial defects with controlled size have been introduced at the surface of fatigue samples. The size of the defect is characterised by the  $\sqrt{area}$  parameter [1]. To relax the residual stresses occurring during the specimen preparation, all the samples underwent a tempering at 500 °C during one hour under vacuum.

## FATIGUE INITIATION MECHANISMS

SEM observations have been done to understand fatigue mechanisms of defect free and defective material under fatigue loading.

### Defect Free Material

#### Crack initiation

Figure 1 shows typical cracks initiated under tension and torsion loadings. The first stage of crack nucleation occurs in the maximum shear plane under both tension and torsion. Then the macroscopic crack that leads to failure of the sample propagates in the plane perpendicularly to the direction of the maximum principal stress (in mode I). Under tension: the stage I crack initiated inside the ferrite grain is very short (1 grain), it branches to stage II directly at the neighbour grain boundary which seems to be the most important microstructural barrier for this material .

Under torsion : the stage I crack can propagate in several grains before branching into mode I and stage II. This is a major difference with stage I propagation under tension. The pearlite bands are preferential sites of branching but the role of this microstructural barrier is different from tension to torsion [ 2].

#### Crack propagation

Before examining the crack propagation, it is useful to define the number of cycles of crack initiation. The crack is initiated inside a ferrite grain then it branches in the neighbour grain boundary which seems to be the most important microstructural barrier for this material. In this section, for defect free materials, we define the number of cycles for crack initiation by the number of cycles necessary to create a crack which exceed this barrier. It seems to be a crack length of 60 µm in surface (1 ferrite grain size + 2\* pearlite grain size).

Table 2 summarise tests and observations carried out in tension and torsion just above the fatigue limit of the material. The following equation is used to calculate the phase of fatigue life propagation (Np(%)):

$$Np(\%) = \frac{N_f - N_i}{N_f} * 100 \quad (1)$$

where  $N_f$  is the number of cycles to failure and  $N_i$  is the number of cycles of crack initiation.

Defect free material shows an early crack initiation particularly in the case of torsion loading.

## Defective Material

### Crack initiation around defect

Figure 2 presents cracks around defects just above the fatigue limit under tension and torsion loadings. The first stage of crack nucleation at the tip of the defect occurs in the maximum shear plane and in the maximum loaded part of the defect under both tension and torsion loadings. Then the macroscopic crack that leads to failure of the sample propagates in the plane perpendicularly to the direction of the maximum principal stress (in mode I). Once this crack is initiated (inside one grain, or maybe two), it branches to stage II without propagating on a longer distance in stage I. Thus, the length of those stage I cracks is always very short.

### Fatigue life propagation

In this section, for defective materials, we define the number of cycles of crack initiation by the number of cycles necessary to create a continuous crack that totally encircles the defect. Figure 3 shows a SEM view of cracks immediately initiated in a 300  $\mu\text{m}$  defect in under tension and torsion.

Figure 4 presents experimental fatigue curves for the crack initiation and for failure of a 300  $\mu\text{m}$  defected material. The stress amplitude is plotted versus of cycles to crack initiation and to failure.

## DISCUSSIONS AND CONCLUSIONS

According to the previous illustration, we assume that initiation mechanisms at defective material are the same as defect free material: the initiation of cracks is done in the slip system where the shear part of the stress tensor is maximum and the propagating plane is always perpendicular to the maximal principal stress direction.

For defective material, we have observed that once the crack is initiated (inside one grain, or maybe two), it branches to stage II without propagating on a longer distance in stage I. Thus, the length of those stage I cracks is always very short. The comparison of Fig. 1 (a) and Fig. 2 (a) illustrates the big difference of stage I cracks between the defective (10~20 $\mu\text{m}$ ) and the defect free material (200~300 $\mu\text{m}$ ) for torsion loading.

It's observed that crack propagation regime life in defect materials is very short, contrary to defect free material which shows an early crack initiation. However the fatigue life initiation is not consumed in defective material, particularly in torsion loading.

## REFERENCES

- [1] Y. Murakami, M. Endo: "The  $\sqrt{\text{area}}$  parameter model for small defects and non metallic inclusions in fatigue strength: experimental evidences and applications" Actes de "Theoretical concepts and numerical analysis of fatigue"; EMAS, Blom A.F., Beevers C.J. Éditeurs, Birmingham, UK, pp. 51-71, 1992.

- [2] T. Billaudeau, Y. Nadot, G. Bezine : « Multiaxial fatigue limit for defective materials: mechanisms and experiments”. Acta materialia 52 (2004) 3911-3920.
- [3] L. Flaceliere, F. Morel, A. Dragon : « Competition between mesoplasticity and damage under HCF – Elasticity/damage shakedown concept.” Int.Jour. Fatigue V 29, 12, December 2007, P. 2281-2297.
- [4] Endo M., Ishimoto I. : « The fatigue strength of steels containing small holes under out-of-phase combined loading”. International Journal of Fatigue 28 (2006) 592–597
- [5] MURAKAMI Y., « Metal Fatigue : effects of small defects and nonmetallic inclusions”, Elsevier editor, 2002.
- [6] NADOT Y., MENDEZ J. and RANGANATHAN N., « Fatigue life assessment of nodular cast iron containing casting defects”, Int J. Fatigue, 26, 311-319, 2004
- [7] NADOT Y. and BILLAUEAU T., « Multiaxial fatigue limit criterion for defective materials », Eng. Fract. Mech., Vol. 73, No. 1 , pp. 112-133, 2006.

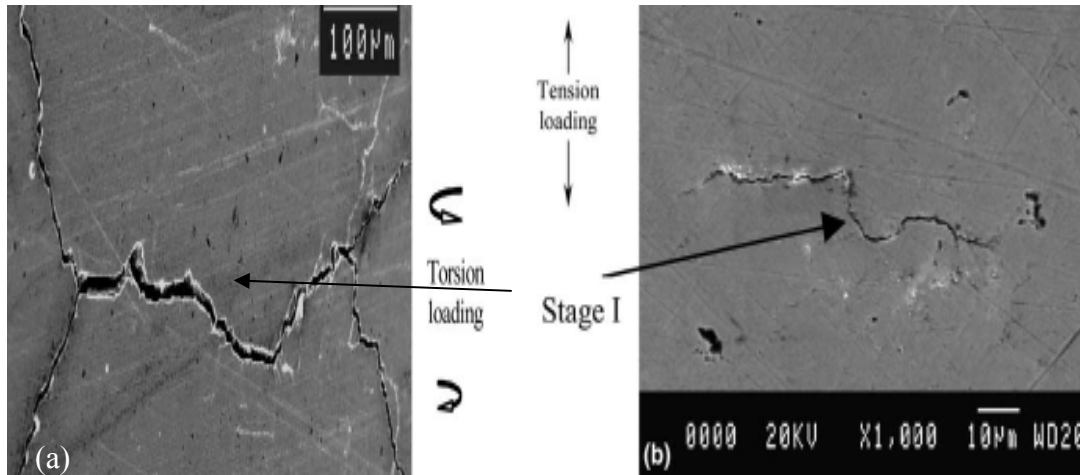
**Tables**

**Table 1** : Mechanic characteristics of the C35 steel

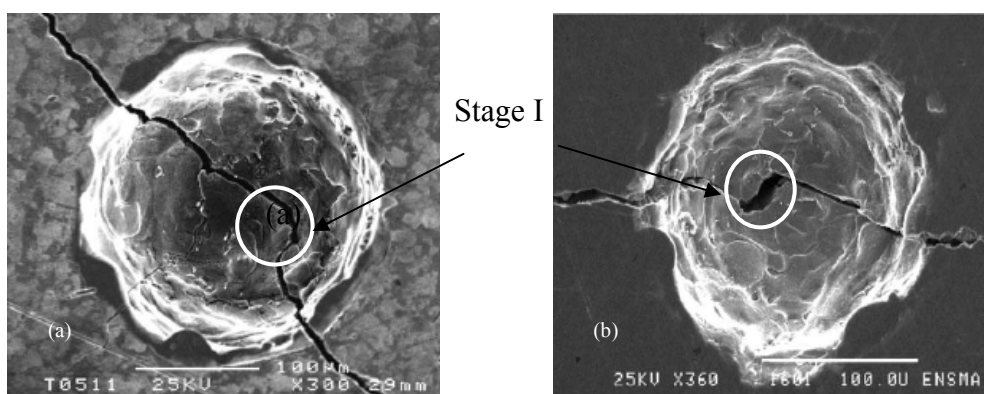
| Young modulus,<br>E (GPa) | R <sub>p0,2</sub> monotonous<br>(MPa) | R <sub>p0,2</sub> cyclic (MPa) | R <sub>m</sub> (MPa) | A%  |
|---------------------------|---------------------------------------|--------------------------------|----------------------|-----|
| 205                       | 350                                   | 280                            | 580                  | 30% |

**Table 2** : Summarising of tests for defect free material

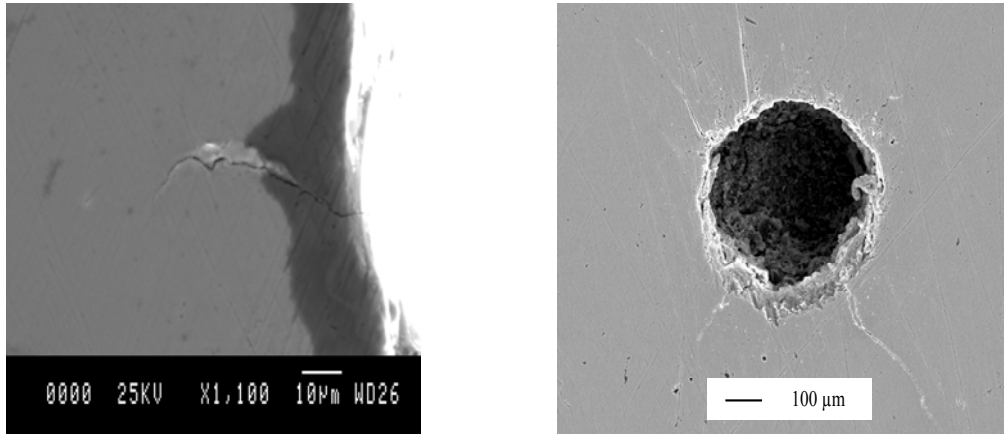
| Fatigue limit<br>(MPa) | Stress<br>amplitude<br>(MPa) | Initiation<br>number of<br>cycles | Failure<br>number of<br>cycles | Fatigue life<br>propagation (%) |
|------------------------|------------------------------|-----------------------------------|--------------------------------|---------------------------------|
| 240 (Tension)          | 250                          | 5*10 <sup>5</sup>                 | 8.13*10 <sup>5</sup>           | 23                              |
| 169 (Torsion)          | 175                          | 3*10 <sup>5</sup>                 | 9.1*10 <sup>5</sup>            | 67                              |



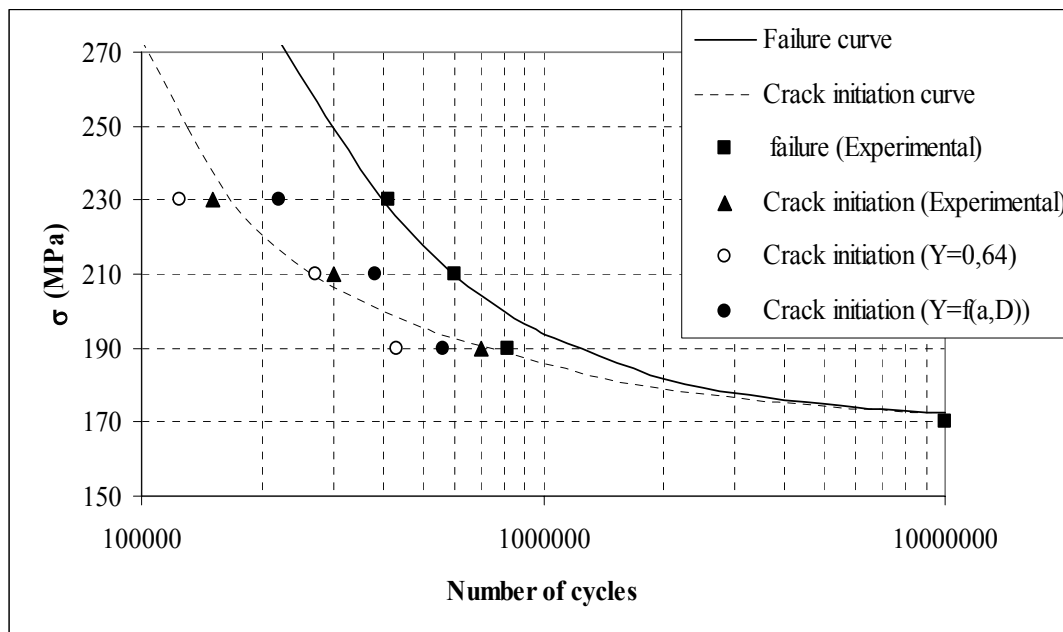
**Fig. 1.** Typical micro-cracks observed above the fatigue limit : a) torsion loading b) tension loading

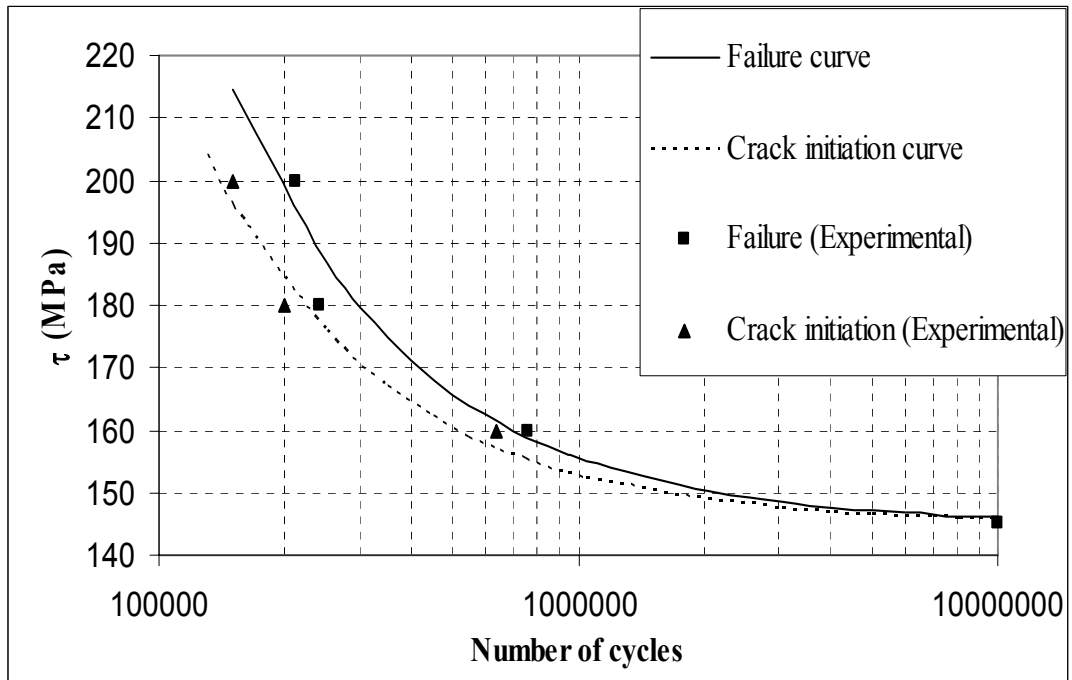


**Fig. 2.** Crack path around defect under loading close to the fatigue limit : (a) 165 µm spherical defect, torsion ( $\tau = 155$  MPa,  $N = 4.7 * 10^6$  cycles), (b) 160 µm spherical defect, tension ( $\sigma = 200$  MPa,  $N = 2 * 10^6$  cycles).



**Fig 3.** SEM view of fatigue crack initiation : a) tension loading after  $7 \cdot 10^5$  cycles ( $N_f = 8.15 \cdot 10^5$  cycles,  $\sigma = 190$  MPa,  $\sigma_D = 170$  MPa), b) torsion loading after  $640 \cdot 10^3$  cycles ( $N_f = 756 \cdot 10^3$  cycles,  $\tau = 160$  MPa,  $\tau_D = 145$  MPa).





(b)

Fig. 4. Experimental data and predicted Wöhler curves : a) tension loading; b) torsion loading ( $\sqrt{\text{area}}=300\mu\text{m}$ )